The ionic KAl_{13} molecule: A stepping stone to cluster-assembled materials

W.-J. Zheng, O. C. Thomas, T. P. Lippa, S.-J. Xu, and K. H. Bowen, Jr.[a)]
Department of Chemistry and Department of Materials Science, Johns Hopkins University, Baltimore, Maryland 21218

(Received 30 January 2006; accepted 13 February 2006; published online 11 April 2006)

Theoretical calculations by Khanna and Jena predicted KAl_{13} to be an ionically bonded, cluster-assembled "diatomic molecule," i.e., $K^+Al_{13}^-$. We have conducted both mass spectral and anion photoelectron spectroscopic studies on KAl_n^-, finding a "dip" at $n=13$ in both their mass spectrum and in their electron affinity versus n trend. While these largely qualitative results are consistent with KAl_{13} being a salt, they can also be explained in terms of the shell model and thus, by themselves, are not conclusive. Quantitative comparisons between calculated photodetachment transition energies and the photoelectron spectrum of KAl_{13}^-, however, allow a strong case to be made for ionic bonding in KAl_{13}. As a prototype for ionic bonding involving intact Al_{13}^- subunits, KAl_{13} may be a stepping stone toward forming ionic, cluster-assembled materials. © *2006 American Institute of Physics*. [DOI: 10.1063/1.2184316]

The discovery of fullerenes in molecular beams[1] and their subsequent preparation in bulk quantities[2] inspired speculation that it might be possible to do the same in other systems as well.[3] Such cluster-assembled materials would consist, in whole or in part, of specific size aggregates which were so stable that they could form macroscopic samples without coalescing with one another and losing their individual identities. The discovery of metcars, again in beams, gave further impetus to this idea and made clear the potential for tailoring specific properties.[4] (The basic metcar unit is M_8C_{12}, where M is an atom of one of several transition metals.) In this regard, another remarkable cluster species to make its debut was Al_{13}^-. The Al_{13}^- cluster anion is unusually stable, exhibiting both electronic and geometric bases for its stability. Electronically, Al_{13}^- has 40 valence electrons, and 40 is a closed shell, magic number in the electronic shell model,[5] where the motion of the delocalized valence electrons is governed by the smeared-out positive potential of the remaining aluminum cations. Structurally, the theory by Khanna and Jena[6] found Al_{13}^- to be an icosahedron with one aluminum atom in the center and twelve at its icosahedral vertices. The combination results in an unusual stability and thus inertness. This was dramatically demonstrated in etching experiments by Leuchtner *et al.*[7] in which a wide range of Al_n^- cluster sizes were subjected to attack by oxygen. There, only Al_{13}^- was left intact, while the other sizes were reacted away. Another impressive demonstration of its stability was provided by Li *et al.*[8] who measured the adiabatic electron affinity of Al_{13} by photodetaching electrons from a beam of Al_{13}^- cluster anions. They found its electron affinity to be 3.6 eV, essentially the same value as that of a chlorine atom. The theory by Dolgounitcheva *et al.*[9] concurred.

The term magic clusters is often used to describe clusters (or species that were born in cluster-forming environments) which exhibit exceptional stability. The sizes and stabilities of the three best known magic clusters, C_{60}, M_8C_{12}, and Al_{13}^-, are compared in Fig. 1. The unique stability of each of these species depends on them possessing their full complement of atoms. Take one atom away, and they loose their special stability, i.e., every atom counts. Thus, one measure of their stabilities is the energy required to remove a single atom from a given cluster, $E(n\rightarrow n-1)$,[10] since this is the energy required to trigger the demise of its unique stability. By showing these values to be comparable, Fig. 1 demonstrates that Al_{13}^- is a legitimate member of the magic cluster club.

Because Al_{13}^- has a icosahedral nuclear framework enveloped in a cloud of delocalized valence electrons, it can be visualized as a negatively charged, nearly a spherical object having the same electron binding energy as Cl^-. This realization led Khanna and Jena[11] to wonder if Al_{13}^- could serve the same role that Cl^- does in an ionic K^+Cl^- molecule. If so, the species thus formed, KAl_{13}, might appear to be a mixed metal cluster, but would instead be the cluster-assembled, ionically bonded "diatomic molecule," $K^+Al_{13}^-$. Extensive calculations by these investigators showed this to be the case. KAl_{13} was found to be a salt molecule, with K^+ ionically bonded to an intact Al_{13}^- cluster anion moiety and with an alkali halide-like dipole moment of ~11 D.[12]

The prospect of forming a macroscopic ionic lattice based on K^+ and Al_{13}^- subunits is an intriguing route to cluster-assembled materials. Since Al_{13}^- is a charged magic cluster, it would require an appropriate counterion in order to form an extended ionic lattice. The calculations by Liu *et al.*,[13] however, suggest that the alkali cations are not large enough to give rise to a stable lattice. It appears that larger cations will have to be utilized if ionic, cluster-assembled materials containing Al_{13}^- subunits are to be realized. Nevertheless, $K^+Al_{13}^-$ molecules, as well as their other alkali siblings, remain invaluable as prototypes for ionic bonding involving intact Al_{13}^- cluster ions. These systems are, in fact, stepping stones to forming ionic, cluster assembled materials composed of Al_{13}^- subunits and appropriate cations, and ex-

[a)]Electronic mail: kitbowen@jhu.edu

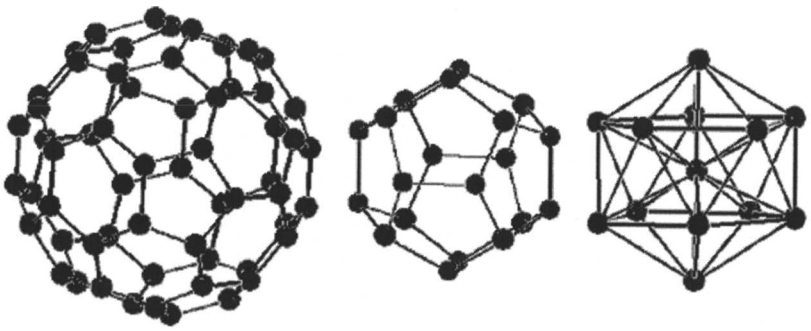

Magic Cluster	C_{60}	Ti_8C_{12} Met-car	Al_{13}^-
Diameter, Å	7.0	5.0	5.4
E(n→n-1), eV	~7	~7	4.7

E(n→n-1) = Energy needed to remove a single atom from the cluster.

FIG. 1. Comparisons of the sizes and critical energies needed to break their magicities for the three magic clusters, C_{60}, Ti_8C_{12} metcar, and Al_{13}^-.

periments that test the theorists' prediction of ionic bonding in them are therefore important.

Hoshino *et al.* have conducted both mass spectral and photoionization experiments that support the theory's prediction of ionic bonding in MAl_{13} molecules, where M=Na and Cs. They observed an enhanced ion intensity (a peak) for $CsAl_{13}^+$ relative to other $CsAl_n^+$ cluster cations in mass spectra, where cations were formed by photoionization of the *neutral* species present,[14] and a markedly decreased ion intensity (a "dip") for $NaAl_{13}^-$ relative to other $NaAl_n^-$ species in cluster anion mass spectra.[15] In addition, they measured a maximum for the ionization potential of $CsAl_{13}$ relative to the ionization potentials of other $CsAl_n$ species[14] as well as the same implied behavior for $NaAl_{13}$.[16] From these data, they concluded that $CsAl_{13}$ is most probably an ionic molecule with Cs^+ outside of an intact Al_{13}^- cluster anion. These results, however, could also have been equally well interpreted in terms of the shell model without invoking ionic bonding. Thus, while their results are supportive of the $M^+Al_{13}^-$ ionic bonding hypothesis, there also exists an equally valid, alternative interpretation. As will be shown below, some of our results are also subject to this limitation.

In a closely related work, Bukart *et al.*[17] measured the photoelectron spectrum of HAl_{13}^-, finding a large HOMO-LUMO gap. With the aid of calculations, they interpreted their spectra as indicating a highly stable HAl_{13} neutral with a covalent $H-Al_{13}$ bond. Our own work with Al_{13}^--type systems has included the photoelectron spectra of $LiAl_{13}^-$ and $CuAl_{13}^-$ as well as mass spectral studies of $Al_{13}^+(H_2O)_1$. Our results on $LiAl_{13}^-$, combined with available calculations, suggested that $LiAl_{13}$ is ionic, but not strongly so.[18] In the case of $CuAl_{13}^-$, we found a magic number evidence for the shell model level reordering and the substitution of a copper atom for an aluminum atom inside the cluster's icosahedral cage.[19] Furthermore, even though Al_{13}^+ has only 38 valence electrons, $Al_{13}^+(H_2O)_1$ is a magic number among $Al_n^+(H_2O)_1$ cluster cations due to its water molecule providing the Al_{13}^+ moiety access to its lone pairs and thus to a degree of 40 electron, closed shell character.[20] Last, no survey of work on magic cluster behavior in aluminum clusters would be complete without mentioning the work by Bergeron *et al.*[21,22] on $Al_{13}I_x^-$, which behave like polyhalide anions when x is an even number, and on $Al_{14}I_x^-$, which behave like alkaline earths in iodide salts when x is an odd number, as well as the work by Li *et al.*[23] on all-metal, aromatic, MAl_4^- species (M=Li, Na, or Cu) and related systems.[24]

Here, we present our work on the KAl_{13}^- anion and its implications for KAl_{13}, its corresponding neutral. We have focused on this particular system because it is the one for which the theory has provided the most benchmarks for comparison. We have conducted both mass spectral and photoelectron (photodetachment) experiments on KAl_n^-. The mass spectral data were collected with both a quadrupole mass spectrometer and a linear time-of-flight spectrometer. The photoelectron data were recorded on a pulsed, anion photoelectron (magnetic bottle) spectrometer. Anion photoelectron spectroscopy is conducted by crossing a mass-selected negative ion beam with a fixed-frequency photon beam and energy analyzing the resultant photodetached electrons. Photodetachment is governed by the energy-conserving relationship $h\nu$=EBE+EKE, where $h\nu$ is the photon energy, EBE is the electron binding energy (the transition energy between the anion and a given state of its corresponding neutral), and EKE is the electron kinetic energy. Our apparatus, which is described elsewhere,[25] consists of a laser vaporization cluster ion source, a linear time-of-flight mass spectrometer, a mass gate, a momentum decelerator, a Nd:yttrium aluminum garnet (YAG) laser operated at 355 nm (3.49 eV/photon) for photodetachment, and a magnetic bottle electron energy analyzer with a resolution of ~35 meV at EKE=1 eV. KAl_n^- cluster anions were generated in a Smalley-type laser vaporization source modified to accept a small oven in its base just below a rotating, translating aluminum rod. Laser ablation of the potassium-coated rod was accomplished with 532 nm (2.33 eV/photon) light pulses from a second Nd:YAG laser, and helium gas was utilized in the pulsed valve.

Figure 2 presents a typical mass spectrum produced with this source. Two interwoven series are seen, one for Al_n^- and the other for KAl_n^-. The magic cluster, Al_{13}^-, is seen as a prominent peak. The KAl_n^- ion intensity rises gradually with n up through n=12, after which it drops precipitously at

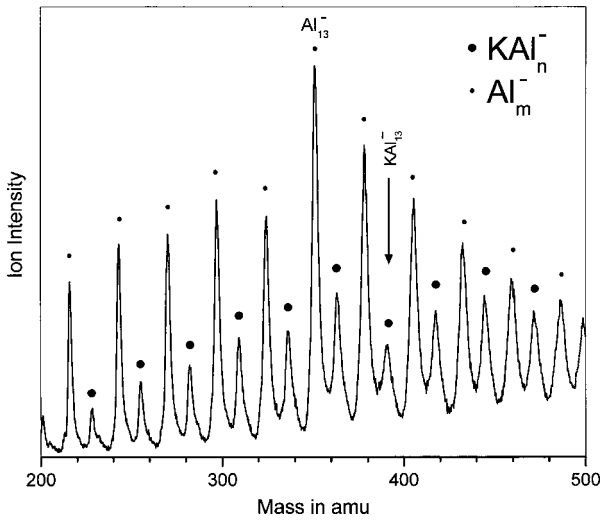

FIG. 2. Mass spectrum showing relative intensity trends for the Al_m^- and the KAl_n^- series.

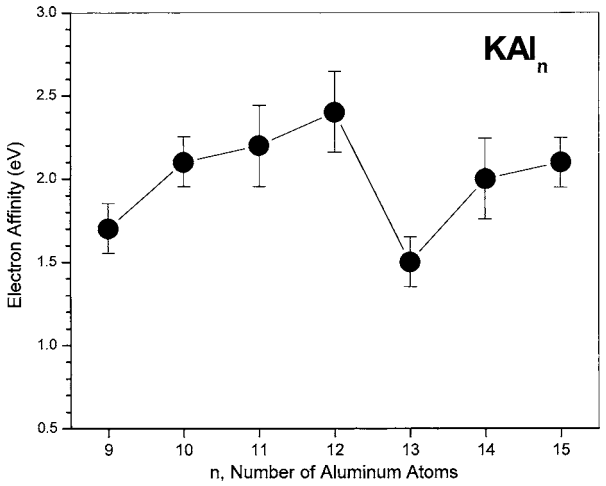

FIG. 3. Plot of KAl_n electron affinities EA vs cluster size n.

KAl_{13}^- before rising again for $n=14$ and 15 and then decreasing thereafter. The dip at KAl_{13}^- can be interpreted in two ways. (1) If most KAl_n clusters are simply mixed metal clusters, then it is not unreasonable that a different amount of KAl_{13} might be present if it is bonded differently, i.e., as a salt, and this would be reflected in its relative ion intensity. (2) A more compelling interpretation, however, comes from the shell model. Neutral KAl_{13} is a 40 valence electron, closed shell in the shell model. As a neutral, it should be abundant because of its closed-shell-based stability, and it should appear as a maximum in an abundance spectrum. Hoshino *et al.* observed this when they photoionized neutral $CsAl_n$ clusters and observed a prominent peak for $CsAl_{13}^+$ in the resulting mass spectrum. As an anion, however, KAl_{13}^- has one extra electron beyond the shell closing magic number at 40, i.e., it has 41 valence electrons. Typically, in shell model systems, there is a substantial loss in stability and abundance when such a system goes one electron beyond its closed shell, magic number of electrons. In some cases, the abundance pattern appears as a shelf, with the species with one too many electrons lying at its foot, while in others, as seen here, this species manifests itself as a dip in the intensity trend. Nakajima also observed a dip in his mass spectrum of $NaAl_{13}^-$ for the same reason. While all of the mass spectral evidence can be easily explained in terms of the shell model, it is important to realize that the shell model would also be applicable to an ionically bonded $K^+Al_{13}^-$ salt, since it too is a 40 valence electron system. Shell model behavior, as is indeed seen in the mass spectral data, should be expected in KAl_{13}, whether it is just a mixture of potassium and aluminum metal atoms or an ionically bonded, salt molecule.

The photoelectron spectra of KAl_n^- were recorded for $n=9-15$ and their corresponding adiabatic electron affinities (EAs) extracted from the spectral regions slightly above their signal thresholds. The electron affinities of homogeneous aluminum clusters, Al_n, are well known from the work of Li *et al.*,[8] and in the $n=9-15$ size range, they tend to be relatively constant at ~2.7 eV except for $n=13$, where the EA is 3.6 eV. It is also known that doping metal clusters with alkali atoms tends to reduce their electron affinity values by several tenths of an electron volt. Thus, from a purely empirical perspective, one might have anticipated a fairly flat EA versus n trend for simple mixed metal KAl_n clusters over this size range, except at $n=13$, where its EA might have been expected to remain larger than the others. The electron affinity values determined from our photoelectron spectra are plotted versus the cluster size in Fig. 3. While most of the EA data points are similar valued and roughly follow the expectations mentioned above for mixed metal clusters, the EA value for $n=13$ does not. There is a sharp decrease in the EA versus n plot at $n=13$, in contrast with the above expectation. Clearly, there is something special about KAl_{13}.

Next, we consider two explanations for the dip in the EA versus n trend at $n=13$ in Fig. 3. In studying the electron affinities of alkali halide salts, Miller *et al.*[26] found them to lie in the range of 0.4–0.9 eV, i.e., they are relatively small. So, to the extent that KAl_{13} mimics an alkali halide salt, one should expect its electron affinity to be small and to stand out prominently as a dip among its neighboring sized, higher electron affinity KAl_n mixed metal clusters in an EA versus n plot, and it does. Using the empirical relationship which correlates alkali halide electron affinities with alkali atom polarizabilities and alkali halide internuclear separations and utilizing the theoretically calculated value for the ionic radius of Al_{13}^-, one can estimate that the electron affinity of KAl_{13} should be ~1 eV. The adiabatic electron affinity that we measured for KAl_{13} is 1.5 eV. While these EA values are not identical, they are in a similar range, and the difference between them may simply be due to the imperfect analogy between ionically bonded KAl_{13} and alkali halides.

The other explanation for the dip in the EA versus n trend is based on the shell model. While neutral KAl_{13} is a 40 valence electron, closed shell species, the KAl_{13}^- anion is a 41 valence electron system. In the shell model, the next available (empty) level beyond the uppermost occupied level of a closed shell is a larger-than-usual step up in energy and therefore is closer to the ionization limit. The 41st valence electron in KAl_{13}^- resides in such an elevated level and thus can be relatively easily removed (photodetached). This elec-

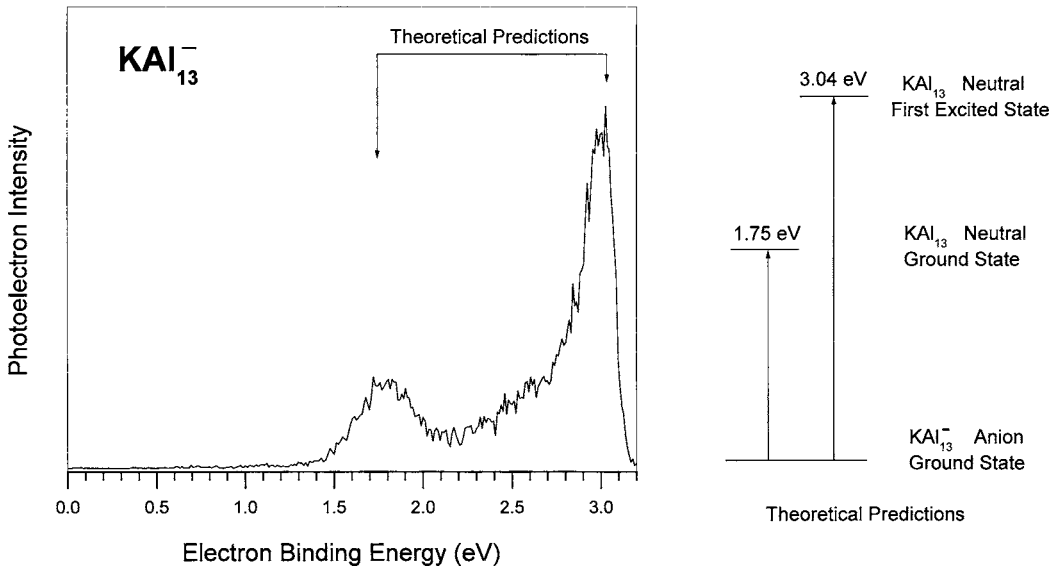

FIG. 4. Photoelectron spectrum of KAl_{13}^- along with theoretical predictions for its first two photodetachment transition energies.

tron's low binding energy translates into a low electron affinity for the anion's corresponding neutral. Closed shell, neutral species generally have reduced electron affinities. Anions whose corresponding neutrals are not closed shells are much less subject to this effect. Thus, the shell model can easily explain the dip at $n=13$ in the EA versus n plot presented in Fig. 3. These considerations also explain the ion intensity dip for anions of closed shell neutrals in mass spectra, i.e., it is energetically less favorable to form them. Likewise, Nakajima and Kaya's observation of maxima for the ionization potentials (IPs) of $CsAl_{13}$ and $NaAl_{13}$ relative to the ionization potentials of other $CsAl_n$ and $NaAl_n$ species can be explained in terms of the shell model. $CsAl_{13}$ and $NaAl_{13}$ are both closed shell neutrals and as such their uppermost occupied shell levels are stabilized and lowered in energy, placing them further down in energy from the ionization limit. This results in a maximum for the ionization potential of the closed shell species. These ionization potential maxima in IP versus n plots are the shell model, flipsides of the electron affinity minimum that we observed in the EA versus n plot for KAl_{13}. Our mass spectral evidence and our anion photoelectron results are complementary to the mass spectral evidence and neutral photoionization results of Nakajima and Kaya, and both can be explained in terms of the shell model. The applicability of the shell model, however, does not preclude KAl_{13} from also being a salt, and both the salt and the shell model explanations for the dip in the EA versus n plot at $n=13$ are probably valid. Below, we will see additional evidence that points in that direction.

The qualitative evidence provided by discontinuities in EA versus n and IP versus n plots at $n=13$ is supportive of ionic bonding in these systems, but since there is also an alternative explanation, it is not conclusive. To further tighten the ring of evidence around this problem, *quantitative* comparisons are needed between experiment and theory. Ashman *et al.*[27] took up this problem and calculated photodetachment transition energies, in part, so they could be compared with our photoelectron spectra of KAl_{13}^-. The first two electronic transitions fell into our experimental range, i.e., from the doublet, ground state of KAl_{13}^- anion to the singlet, ground state of KAl_{13} neutral and from the doublet, ground state of KAl_{13}^- anion to the triplet, first excited state of KAl_{13} neutral. At our request, they calculated both the adiabatic electron affinity of KAl_{13} and the vertical detachment energies (VDEs) of both transitions. The VDE corresponds to the electron binding energy for the maximum overlap between the anion's wave function and the neutral potential surface above it in a vertical photodetachment transition, and for this reason, VDE values correspond to the electron binding energy of spectral peak maxima. Figure 4 displays the photoelectron spectrum of KAl_{13}^-. One observes two peaks, the maxima of which are separated by 1.29 eV. The calculation of Ashman *et al.* predicts the VDE of the KAl_{13}^- ground state-to-KAl_{13} ground state transition to be 1.75 eV and the KAl_{13}^- ground state-to-KAl_{13}^- excited state transition to be 3.04 eV. The electron binding energies of both of these transitions are marked on our spectrum in Fig. 4, and it can be seen that the agreement is excellent. Also, their calculated value for the adiabatic electron affinity is 1.54 eV, whereas our measured EA value is 1.5 ± 0.1 eV. The energy separation between the two peaks in the spectrum corresponds to the HOMO-LUMO gap (also the singlet-triplet splitting) of neutral KAl_{13} at the geometry of its anion, KAl_{13}^-. Given that theory found relatively little structural difference between the KAl_{13}^- anion and its corresponding neutral, KAl_{13} (a finding that is echoed by the small difference between EA and the lowest VDE transition energy), the measured HOMO-LUMO gap energy of 1.29 eV is probably a good estimate for the adiabatic HOMO-LUMO gap in neutral KAl_{13} (although there is some uncertainty since the structure of the first excited state of KAl_{13} is not known). More importantly, however, is the observation that the HOMO-LUMO gap in KAl_{13} is rather large, since this implies that KAl_{13} is nonmetallic, i.e., KAl_{13} is not simply a mixture of metal atoms with metallic bonding. The calculations have been definitive in their finding of strong ionic

bonding in KAl_{13}, and the close correspondence between the quantitative theoretical predictions and our experimental results makes a strong case for definitively concluding that KAl_{13} is an ionically bonded, cluster-assembled, "diatomic molecule."

This work was supported by the Division of Materials Science and Engineering, Office of Basic Energy Sciences, U.S. Department of Energy under Grant No. DE-FG0295ER45538. Acknowledgment is also made to the Donors of The Petroleum Research Fund, administered by the American Chemical Society, for partial support of this research under Grant No. 28452-AC6.

[1] H. W. Kroto, J. R. Heath, S. C. O'Brian, R. F. Curl, and R. E. Smalley, Nature (London) **318**, 162 (1985).
[2] W. Kratschmer, L. D. Lamb, F. Fostiropoulos, and D. R. Huffman, Nature (London) **347**, 354 (1990).
[3] S. N. Khanna and P. Jena, Phys. Rev. Lett. **69**, 1664 (1992).
[4] B. C. Guo, K. P. Kerns, and A. W. Castleman, Science **255**, 1411 (1992).
[5] W. D. Knight, K. Clemenger, W. A. de Heer, W. A. Saunders, M. Y. Chou, and M. L. Cohen, Phys. Rev. Lett. **52**, 2141 (1984).
[6] S. N. Khanna and P. Jena, Chem. Phys. Lett. **219**, 479 (1994).
[7] R. E. Leuchtner, A. C. Harms, and A. W. Castleman, J. Chem. Phys. **91**, 2753 (1989).
[8] X. Li, H. Wu, X.-B. Wang, and L.-S. Wang, Phys. Rev. Lett. **81**, 1909 (1998).
[9] O. Dolgounitcheva, V. G. Zakrzewski, and J. V. Ortiz, J. Chem. Phys. **111**, 10762 (1999).
[10] D. E. Bergeron, A. W. Castleman, T. Morisato, and S. N. Khanna, J. Chem. Phys. **121**, 10456 (2004).
[11] S. N. Khanna and P. Jena, Phys. Rev. B **51**, 13705 (1995).
[12] S. N. Khanna, B. K. Rao, and P. Jena, Phys. Rev. B **65**, 125105 (2002).
[13] F. Liu, M. Mostoller, T. Kaplan, S. N. Khanna, and P. Jena, Chem. Phys. Lett. **248**, 213 (1996).
[14] K. Hoshino, K. Watanabe, Y. Konishi, T. Taguwa, A. Nakajima, and K. Kaya, Chem. Phys. Lett. **231**, 499 (1994).
[15] A. Nakajima, K. Hoshino, T. Sugioka, T. Naganuma, T. Taguwa, Y. Yamada, K. Watanabe, and K. Kaya, J. Phys. Chem. **97**, 86 (1993).
[16] A. Nakajima, K. Hoshino, T. Naganuma, Y. Sone, and K. Kaya, J. Chem. Phys. **95**, 7061 (1991).
[17] S. Burkart, N. Blessing, B. Klipp, J. Mueller, G. Gantefoer, and G. Seifert, Chem. Phys. Lett. **301**, 546 (1999).
[18] O. C. Thomas, W.-J. Zheng, T. P. Lippa, S.-J. Xu, S. A. Lyapustina, and K. H. Bowen, J. Chem. Phys. **114**, 9895 (2001).
[19] O. C. Thomas, W.-J. Zheng, and K. H. Bowen, J. Chem. Phys. **114**, 5514 (2001).
[20] T. P. Lippa, S. A. Lyapustina, S.-J. Xu, O. C. Thomas, and K. H. Bowen, Chem. Phys. Lett. **305**, 75 (1999).
[21] D. E. Bergeron, A. W. Castleman, T. Morisato, and S. N. Khanna, Science **304**, 84 (2004).
[22] D. E. Bergeron, P. J. Roach, A. W. Castleman, N. O. Jones, and S. N. Khanna, Science **307**, 231 (2005).
[23] X. Li, A. E. Kuznetsov, H.-F. Zhang, A. I. Boldyrev, and L.-S. Wang, Science **291**, 859 (2001).
[24] X. Li and L.-S. Wang, Phys. Rev. B **65**, 153404 (2002).
[25] W.-J. Zheng, J. M. Nilles, O. C. Thomas, and K. H. Bowen, J. Chem. Phys. **122**, 044306 (2005).
[26] T. M. Miller, D. G. Leopold, K. K. Murray, and W. C. Lineberger, J. Chem. Phys. **85**, 2368 (1986).
[27] C. Ashman, S. N. Khanna, and M. R. Pederson, Phys. Rev. B **66**, 193408 (2002).